



# Chemical Engineering Design Projects 4:

## CHEE10002

---

Volume II: Design of a fluidised bed reactor for the conversion of polysilicon via monosilane

Max Milarvie

S1711125

31/03/2021

### Contents

i. Nomenclature list .....	3
ii. COVID-19 Impact statement .....	4
1. Design Requirements and Specifications .....	4
1.1. Introduction .....	4
1.2. Constraints and Assumptions .....	4

1.3. Alternatives .....	5
2. Process Flowsheet, Material & Energy Balances .....	8
2.1. Process Flowsheet .....	8
2.2. PFD description.....	11
3. Equipment Selection & Sizing .....	12
3.1. Shortcut methods.....	12
3.2. Design summary .....	14
3.3. Implications of shortcut design .....	20
3.4. Alternative arrangements .....	20
4. Operation of equipment and control, Start-up & Shutdown.....	20
4.1. Description of normal operation, start-up and shutdown .....	20
4.1.1. Commissioning and Pre-Commissioning.....	20
4.1.2. Start-up .....	21
4.1.3. Normal Operation.....	21
4.1.4. Shut Down.....	21
4.2. Control strategy .....	22
4.2.1. Flowrate Control .....	22
4.2.2. Level Control.....	23
4.2.3. Composition Control .....	23
4.2.4. Temperature Control.....	23
4.2.5. Pressure Control .....	23
4.3. Safety systems & Fugitive emissions .....	23
5. Critical Review of Design .....	25
5.1. Shortcut design performance.....	25
5.2. Operability beyond flowsheet specifications.....	25
5.3. Limitations of shortcut design .....	26
5.4. Sensitivity of shortcut design .....	26
5.5. Accurate methods for design .....	27
5.6. Group dynamic and characteristics.....	28
6. References.....	28
7. Appendices .....	31
Appendix A – Shortcut Calculation .....	31
Appendix B – Start-up, Shutdown and Normal Operation Sequences .....	40

## i. Nomenclature list

Table 1: List of nomenclature used

Nomenclature	Meaning
CAD	Computer Aided Design
CAPEX	Capital expenditure
CFD	Computational fluid dynamics
$C_p$	Specific heat capacity
$d_b$	Bubble diameter
$d_{b0}$	Bubble diameter formed on entry above distribution plate
$d_{bm}$	Maximum bubble diameter in the column
$d_p$	Particle diameter
$D_t$	Diameter of the reactor bed
$g$	Gravitational constant
$H$	Enthalpy
$K$	Equilibrium Constant
$k$	Kinetic parameter
OPEX	Operational expenditure
PFD	Process flow diagram
PFR	Plug flow reactor
R&D	Research and development
$Re$	Reynold's Number
$r_g$	Rate of growth
SWOT	Strengths, Weaknesses, Opportunities and Threats
TCS	Trichlorosilane
$u_0$	Operational velocity of the gas
$u_b$	Bubble velocity
$u_{br}$	Single bubble velocity
$u_e$	Velocity of the gas in emulsion phase
$u_{mf}$	Minimum fluidisation velocity of the gas
$u_{ms}$	Minimum slugging velocity of the gas
$u_s$	Velocity of the moving solids phase
$u_t$	Free-fall terminal velocity of particle
$v_o$	Volumetric flow of gas through the column

X	Conversion
$\alpha$	Wake parameter
$\gamma$	Volume of catalyst in phase
$\delta$	Volume fraction of bubbles in the column
$\epsilon_{mf}$	Porosity of bed at minimum fluidisation
$\mu$	Viscosity
$\rho_c$	Density of the solid phase
$\rho_g$	Density of the gas phase
$\psi$	Sphericity

## ii. COVID-19 Impact statement

The COVID-19 outbreak resulted in the design project being made more difficult than in previous years. Along with the impacts noted in the V1 submission, the impact on this submission includes, though is not limited to:

- Access to library resources were difficult, even with the option of scanned chapters of books, this was often still difficult if the pages/chapters within a book were unknown. Books such as Silicon Material Preparation and Economical Wafering Methods by Ralph Lutwack were not available in the library, as such purchased from the USA and had associated delay to design process
- The difficult working environment created delays in the progress of the report, this resulted in long working hours near the end of the project to complete the report on time. As a result, the stress caused by submission was significantly higher than expected.
- Some issues with connection to the university VPN created issues accessing UniSim and other software as well as literature data.

## 1. Design Requirements and Specifications

### 1.1. Introduction

The primary objective of this volume is to evaluate the design of a fluidised bed reactor utilised for the conversion of purified monosilane to polysilicon via chemical vapour deposition onto seed particles of polysilicon. This area of the plant satisfies the main objective for the design of a region of the polysilicon plant; and lies after the synthesis and purification of monosilane, with the purified stream of monosilane and fluidising gas of hydrogen as primary inlet streams. The major outlet streams include the reactor vent gases and polysilicon in granular form, which is sent for further processing by Cz method. The objective of this volume is to consider a shortcut design of a fluidised bed reactor, utilising the Kunii-Levenspiel shortcut design method paired with various literature findings and critically evaluate the feasibility of such shortcut calculations on the final outcome of the design process. A novel method for the setup of fluidised bed reactors for the production of polysilicon is also discussed.

### 1.2. Constraints and Assumptions

There are various constraints which influence decisions for the design of the reactor. Perhaps most importantly is sufficient product purity, which is dependent on various factors including the purity of the inlet reactants. The yearly capacity must also match the nameplate capacity

of the plant, as such a sufficient capacity of reactor design is important. A full set of constraints are tabulated below.

*Table 2: Constraints of design*

<b>Constraint</b>	<b>Reasoning</b>
Polysilicon product purity of electronic grade, 11N pure.	Specified in remit.
Capacity to produce 7840 T per year	Specified in remit based upon nameplate capacity of 2 GW. Based upon literature values [1].
Reactor sizing	Considerations for reactor lining to obtain sufficient product purity dictate the need for a reactor lining, which reduces the maximum permissible diameter of the reactor and results in significantly increased CAPEX.
Electricity costs	Due to current changes with the largest energy provider in South Africa, energy prices are changing causing large changes in future economic predictions [2].
Plant lifetime	A shorter plant lifetime allows less time for the initial plant investment to be recovered and, hence, profit to be made.

To allow for a feasible design of the process to occur, certain global assumptions were made and are tabulated below. More specific assumptions are detailed at the relevant section of the report.

*Table 3: Assumptions of design*

<b>Assumption</b>	<b>Reasoning</b>
Impurities neglected in design.	Polysilicon purity of 11N of negligible quantity or influence.
A plant annual operating time of 8000 hours was assumed, the remainder was taken as planned maintenance.	This is a standard estimated time for operating hours [3]

### 1.3. Alternatives

There exist various options for reactor styles designed to provide epitaxial growth of silicon particles. These are covered in reasonable detail by Lutwack et al [4]. A review of literature was conducted and corresponding SWOT analysis performed, which is tabulated below.

*Table 4 - SWOT Analysis for the Reactor Options*

<b>Process</b>	<b>Strengths</b>	<b>Weaknesses</b>	<b>Opportunities</b>	<b>Threats</b>
<b>Fluidised bed reactor</b>	Continuous process Low OPEX costs due to minimal cooling duty. High seed surface area for deposition Spherical particles formed ease downstream processing	Product purity Fines formation Complex operation with control of multiple variables critical for suitable reactor conditions	Improvement in scavenging of fines resulting in increased feasible product	Dust formation has associated risk of dust explosions Complex fluid dynamics so difficult scale-up from laboratory pilot to industrial scale

Siemens reactor	High product purity Well established, highly optimised technology	Energy cost for heating and cooling of reactor Limited scope for future improvements since developed technology Additional milling stage required before ingot growth due to product morphology Batch process so increased downtime Lower surface area for silane deposition	Market for side products from vent gas	Little scope for retrofitting if process becomes surplus to market requirements
Aerosol reactor	Operates by pyrolysis of silane to make silicon dust at significantly lower temperatures of 450°C	Technology at pilot stage Microstructure of product significantly poorer than conventional epitaxial growth methods	Improvement of scavenging of fines resulting in increased quality of scavenged product microstructure	High dust formation has increased associated risk of dust explosions

The fluidised bed reactor was chosen as the most suitable option. A survey of literature indicated suitable considerations to be made to adapt a traditional FBR for the pyrolysis of monosilane onto silicon seed crystals. These included quartz lining to inhibit homogeneous deposition of silicon onto the reactor walls which influences the economics of the process as it places limitations on the diameter of the reactor, and thus restricting the potential for a single larger reactor and instead introducing the restriction of multiple smaller reactors [5]. The same consideration would apply to both Siemens reactors and aerosol reactors, though the fines production in Siemens bell jar reactor was significantly increased in comparison to a fluidised bed, as such a significantly greater proportion of the feed was lost to a non-desirable side product and without effective fines scavenging this results in an economic loss [6]. Across the range of options for the reactor, there is not a massive range in consideration for the environmental impact of each process. No specific process requires any environmentally damaging materials though the greatest energy cost is taken up by the Siemens reactor due to internal heating of the polysilicon rods and external cooling of the reactor, thus an inefficient usage of energy having an associated increase in duty and various knock-on effects resulting in increased greenhouse gas emissions [5]. Consideration was made for the raw material requirements for each reactor, with very similar requirements for each. The fluidised bed requires an amount of hydrogen to ensure a suitable fluidisation regime, and varying choice of fluidisation gas incurring associated expense. Similar consideration of transporting gas such as hydrogen is required for the Siemens reactor and the aerosol reactor which requires an inert medium such as nitrogen or argon. There was no obvious choice between reactors for the overall raw material cost. Given the volatility of the polysilicon market, it could be hypothesised that a fluidised bed is more future-proofed than a Siemens style bell jar reactor as it has wider utility across various chemical industries such as petrochemical, whereas bell jar and aerosol reactors are rather specific to the polysilicon production process. The range in health and safety is difficult to quantify from literature, though there is constant risk associated with dust formation, which all three reactors produce. The polysilicon industry has had various disasters in recent times, though few are attributed to the reactor, however; minimisation of fines would be desirable. The continuous operation of fluidised bed reactor requires less manual cleaning than the Siemens process inherently requires, thus saving significant expenditure on extra equipment for the purposes of rotation to maintain sufficient output.

There also exists a variety of alternative feedstock options for the fluidised bed including monosilane and TCS primarily which were considered and tabulated below. The author notes other feed options exist, such as DCS, though limited availability of literature hindered the evaluation of a non-established process.

*Table 5: SWOT Analysis of Process Alternatives*

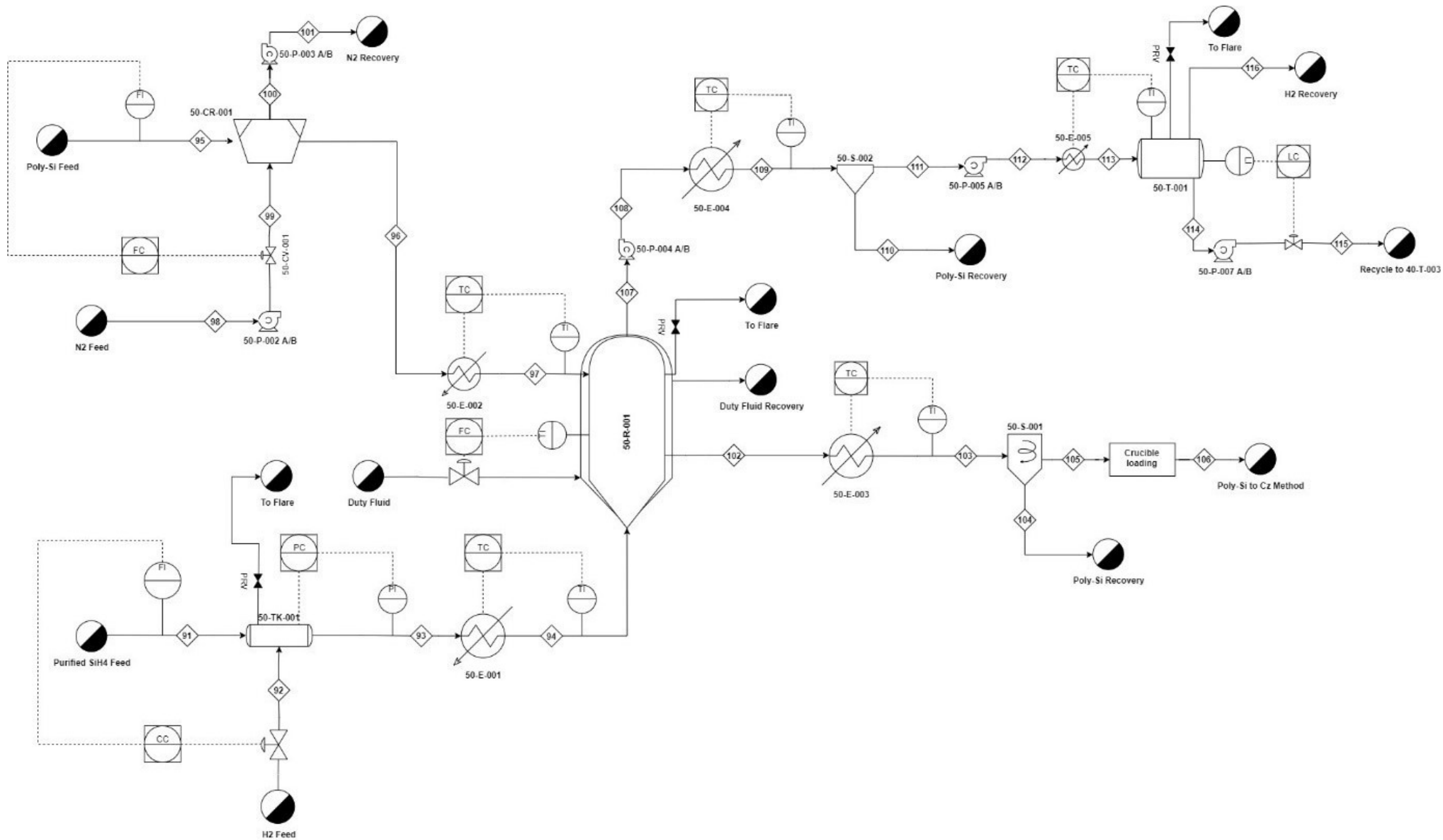
<b>Process</b>	<b>Strengths</b>	<b>Weaknesses</b>	<b>Opportunities</b>	<b>Threats</b>
<b>Silane fed FBR</b>	Operational temperature of 600-800°C Conversion reaction	Fines production	Improvements in fines recombination technology could allow for a reduction in unusable side product	
<b>TCS fed FBR</b>	No synthesis or purification of monosilane required, reducing CAPEX and OPEX.	Increased fines production Operational temperature of 800-1000 °C Corrosive chloride environment Equilibrium reaction	Improvements in fines recombination technology could allow for a reduction in unusable side product	Technology not established and thus there is room for mistakes which may lead to significant losses.

The silane feed was chosen as the most suitable option. A survey of literature indicated the silane fed FBR as significantly more established in industry, with various companies investing in research and development process [7]–[9]. The success of the main pilot TCS-fed FBR operated by Wacker-Chemie has been limited [7]–[9].

2. Process Flowsheet, Material & Energy Balances

2.1. Process Flowsheet

Figure 1: Process Flow Diagram around the fluidised bed reactor, detailed in V1 as area 50 of FBR plant.




	PFD Polysilicon Production - FBR Process		
	Polysilicon FBR Area 50		
	Commissioned by: AGC Technology LLC		
Drawn by: Max Milarvie		Group 11	Revision 1
Date: 21/03/2021	Scale: N/A	Location: Mossel Bay, South Africa	Page: 5/5



Table 6: Material balance for region shown on PFD, calculations provided in V1.

Area 50: Polysilicon Production																											
Stream		91	92	93	94	95	96	97	98	99	100	101	102	103	104	105	106	107	108	109	110	111	112	113	114	115	116
Temperature	°C	55	55	55	300	25	25	650	25	25	25	25	650	25	25	25	25	650	650	25	25	25	25	-145	-145	-145	-145
Pressure	Bar	20	10	10	10	1	1	1	30	30	30	30	1	1	1	1	1	10	10	10	10	10	10	10	10	10	10
Phase		V	V	V	V	S	S	S	V	V	V	V	S	S	S	S	S	V/S	V/S	V/S	S	V	V	V/L	L	L	V
Mass Flow	kg/hr	1474.87256	1758.87002	3233.74258	3233.74258	245	245	245	187.1012	187.1012	187.1012	187.1012	1225	1225	245	980	980	2260.9548	2260.9548	2260.9548	58.9948975	2201.9599	2201.9599	2201.9599	232.154906	232.154906	1969.804994
Molar Flow	kmol/hr	45.9214368	872.507301	918.428738	918.428738	8.72320729	8.72320729	8.72320729	6.678989341	6.678989341	6.678989341	6.678989341	43.6160365	43.6160365	8.72320729	34.8928292	34.89282917	957.266396	957.266396	957.266396	2.10050906	955.165887	955.1658869	955.165887	8.26585864	8.26585864	946.900284
Heat Flow	kJ/hr	1.64E+06	7.45E+05	2.38E+06	1.13E+07	4.23E+05	4.23E+05	5.53E+05	-15.38690356	-15.38690356	-15.38690356	-15.38690356	2.77E+06	2.11E+06	4.23E+05	1.69E+06	1.69E+06	2.72E+05	4.54E+05	-4.31E+07	1.02E+05	3.15E+05	3.15E+05	-4.30E+06	1.02E+05	1.02E+05	-4.52E+06
Si	Mole Fraction	0.0000	0.0000	0.0000	0.0000	1.0000	1.0000	1.0000	0	0	0	0	1.0000	1.0000	1.0000	1.0000	1.0000	0.0022	0.0022	0.0022	1.0000	0.0000	0.0000	0.0000	0.0000	0.0000	0.0000
H2	Mole Fraction	0.0000	1.0000	0.9500	0.9500	0.0000	0.0000	0.0000	0	0	0	0	0.0000	0.0000	0.0000	0.0000	0.0000	0.9882	0.9882	0.9882	0.0000	0.9904	0.9904	0.9904	0.0000	0.0000	0.9990
Silane	Mole Fraction	1.0000	0.0000	0.0500	0.0500	0.0000	0.0000	0.0000	0	0	0	0	0.0000	0.0000	0.0000	0.0000	0.0000	0.0096	0.0096	0.0096	0.0000	0.0096	0.0096	0.0096	1.0000	1.0000	0.0010
Nitrogen	Mole Fraction	0.0000	0.0000	0.0000	0.0000	0.0000	0.0000	0.0000	1	1	1	1	0.0000	0.0000	0.0000	0.0000	0.0000	0.0000	0.0000	0.0000	0.0000	0.0000	0.0000	0.0000	0.0000	0.0000	0.0000
SUM:		1.0000	1.0000	1.0000	1.0000	1.0000	1.0000	1.0000	1.0000	1.0000	1.0000	1.0000	1.0000	1.0000	1.0000	1.0000	1.0000	1.0000	1.0000	1.0000	1.0000	1.0000	1.0000	1.0000	1.0000	1.0000	1.0000

Table 7: Energy Cost over Units shown in PFD, calculations provided in V1.

Equipment Description	Unit	Energy In (kJ/hr)	Energy Out (kJ/hr)
50-R-001 seed furnace	50-E-002	1.30E+05	
50-R-001 product cooler	50-E-003		6.60E+05
50-R-001 product cooler	50-E-004		4.36E+07
Heat exchanger	50-E-005		4.62E+06
Pump	50-P-001A/B	2.25E+05	
Pump	50-P-002A/B	856.7	
Pump	50-P-003A/B	856.7	
Pump	50-P-004A/B	360.5	
Pump	50-P-005A/B	147.6	
Pump	50-P-006A/B	35.97	

TOTAL		3.57E+05	4.89E+07
-------	--	----------	----------

## 2.2. PFD description

### *Area 50 – Polysilicon Fluidised Bed Unit*

The first stream into Area 50, stream 91, is purified monosilane stream from Area 40 and arrives at 55°C and 20 bar as vapour. The fluidised bed requires a specific molar ratio of monosilane to hydrogen at the inlet, controlled by the flow of hydrogen in stream 92, and the hydrogen is added from storage at 10 bar to the monosilane stream in tank 50-TK-001. The pressure of this vessel is influenced by both inlet streams 91 and 92, as such a pressure release valve is on the tank to flare for safety purposes in case of overpressure, and the pressure is controlled by a pressure controller on a control valve on the outlet of the tank. The outlet stream from 50-TK-001, stream 93 is passed through heater 50-E-001 where it is preheated to from 55°C to 300°C, below the pyrolysis temperature of monosilane, and this temperature is monitored for safe operation of the process as exceeding pyrolysis temperature would result in the risk of explosion.

The crushing of polysilicon seed particles occurs at ambient temperature and requires a sufficient flow of pressurised nitrogen, as such the flow of nitrogen, stream 99, is controlled based upon the flow of polysilicon, stream 95 into the crusher unit 50-CR-001. The nitrogen is pressurised to 30 bar, and is recovered after milling in streams 100 and 101. The crushed polysilicon is heated in furnace 50-E-002 to 650°C. Sufficient preheating is required to prevent heat losses across the fluidised bed and is done before the heated seed polysilicon particles are fed into the reactor 50-R-001 by stream 97. Pneumatic transport should be utilised throughout the transport of solid particles where dust or fines exist to minimise the risk of conveyor belts as associated dust explosions.

The reactor has various control loops to ensure maintenance of optimal reactor conditions and necessary safety measures. The temperature of the reactor is controlled through the reactor jacket and the duty fluid heats the reactor in accordance with the temperature feedback control loop. There is a pressure release valve to waste disposal if the fluidised bed becomes over pressured and requires purging, subject to correct environmental regulation for waste disposal.

Solid polysilicon is extracted from the reactor at 650°C in stream 102, and passed through cooler 50-E-003. Sufficient cooling is ensured using a temperature control loop adjusting the controlled variable of flow of cooling duty fluid through 50-E-003. Stream 103 at 25°C is passed through cyclone 50-S-001 to separate the polysilicon crystals with sufficient epitaxial growth and those which are smaller, thus suitable for storage and reuse as seed crystals in stream 104. The polysilicon product of sufficient size are contained in stream 105, and loaded into crucibles before post processing via the Czochralski method.

The vent gases leave the reactor via stream 107 at 650°C and 10 bar, where it is cooled by cooler 50-E-004, again, sufficient cooling is ensured using a temperature control loop adjusting the controlled variable of flow of cooling duty fluid through 50-E-004. There is the opportunity for recovery of this heat across 50-E-003 and 50-E-004 for utilisation in the preheating of stream 93 and 96. The vent gases still contain a mixture of unreacted monosilane, hydrogen and silicon fines, which require separation. The silicon fines are separated over cyclone 50-S002 and collected in stream 110. To separate the hydrogen from the unreacted monosilane for recycling, stream 112 is cooled to –145°C, where at 10 bar, the monosilane will condense and the hydrogen will remain vapour in a flash drum. This cryogenic flash allows for the collection of vapour phase hydrogen to be collected in stream 116, and unreacted liquid phase monosilane to be recycled to 40-TK-003 in stream 115. The level of 50-TK-002 is controlled by manipulating the outlet flow of the monosilane from the vessel.

Although not shown in the PFDs, holdup tanks should be situated throughout the plant between major units. These have been omitted to improve the legibility of the diagrams. Holdup tanks would play an important role in the daily operation of the plant. They ensure that there is adequate feed to maintain steady state in each unit, even if there are disturbances to upstream units. The tanks would not affect the start-up time of the process as they should be bypassed whilst the process reaches steady state.

Perhaps the most major design decision was to utilise a sequence of fluidised bed reactors for incremental growth of polysilicon crystals rather than single size growth across all reactors. The design of this process therefore allows for more specific fluidisation regimes at each particle size, and constant extraction of particles from each reactor passing onto the next reactor in sequence. This decision was made due to the range in the operational gas velocity at a particle size of 100 microns, being massively different to at a particle size of 1000 microns, so a sequence of 8 reactors in equal stages of growth were used to take each seed particle from 100 microns to 1000 microns. This sequence of reactors will not influence product morphology since the same epitaxial growth still occurs but will tailor fluidisation regimes to particle sizes in each respective reactor, leading to optimised reactor conditions and a reduction in deviations towards slugging or fixed bed states.

## 3. Equipment Selection & Sizing

### 3.1. Shortcut methods

There exist various models and shortcut methods for the design of a fluidised bed reactor, with the Kunii – Levenspiel Model with Its Davidson Bubbles and Wakes (K-L model) utilised for the design in this volume due to the applicability, simplified nature and holds no requirement for a computational simulation [10]. The K-L model is sufficient for an estimation of the main features of the reaction including volume fraction of phases, velocities of gases and solids and contacting regimes amongst others, and provides an improvement on the simplistic two-phase model [11]. The method for the shortcut calculation was followed from Yates in Fluidised Bed Reactors: Processes and Operating Conditions [12]. The model is followed for all reactors designed and requires various primary operating conditions. These operating conditions include the fluidising gas, one of the reactants, entering the base of the column and flowing up the column as bubbles. During residence in the column, mass transfer occurs between reactant gas and the surface of the solid seed particles of silicon as the gas diffuses into and out of solid polysilicon surface. The rate of diffusion influences conversion, along with residence time and various parameters associated with the gas phase [12]. The principle of fluidisation in the reactor is detailed to a great extent by Kunii and Levenspiel in Fluidisation Engineering [11].

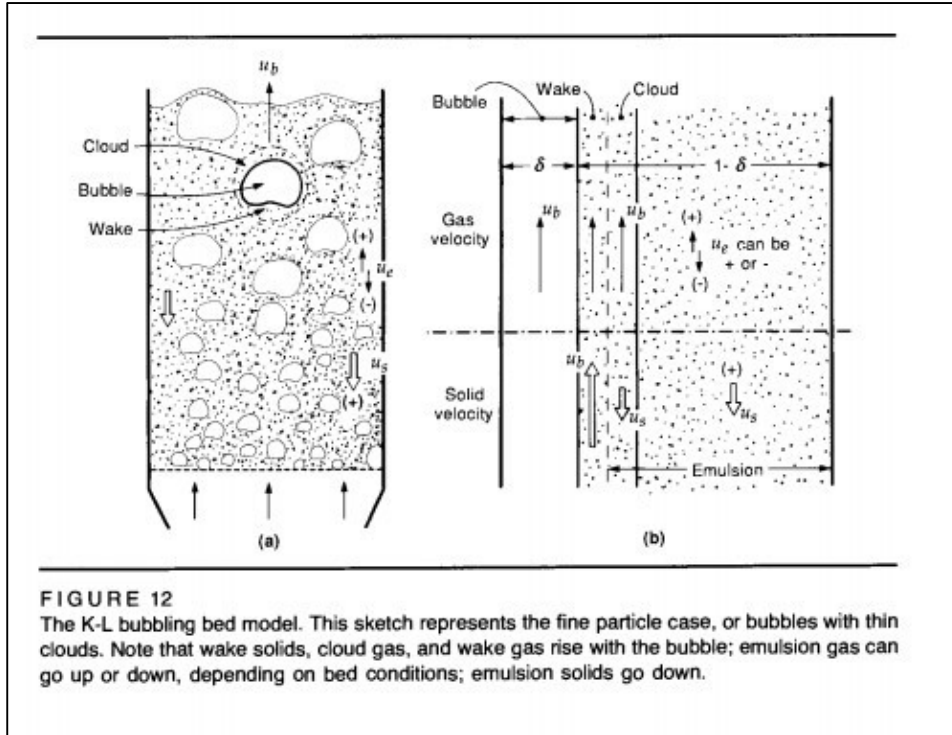
The major assumptions of this model as detailed by Yates are shown in the table below. Note that the bubble phase refers to the bubbles in the column, and the emulsion phase refers to the expanded bed of particles, with the cloud phase referring to the intermediate between the two.

*Table 8: Assumptions for the shortcut design*

Assumption Parameter	Assumption	Reasoning
Geldart Classification of particles	Polysilicon particles behave as Geldart Group B solids.	Particle size ranging from 100 – 1000 $\mu\text{m}$ and particle density of 2.3 $\text{g/cm}^3$ , within $1.4 < \rho_c < 4 \text{ g/cm}^3$ . [11]
Fluidisation regime	Bed operates under a bubbling fluidised state	Maintenance of desirable reactor conditions without the associated risks of slugging.
Bubbles size	Bubbles of uniform size	Assumption of the K-L model [12].
Solids in the emulsion phase	Solids in the emulsion phase act in plug flow downwards	Assumption of the K-L model [12].
Emulsion phase is at minimum fluidising conditions.	Gas occupies equal voidage in emulsion phase irrespective of bubble phase	Assumption of the K-L model [12].
Concentration of solids in bubble wake	Equal to the concentration of solids in emulsion phase. Void fraction in wake equal to $\epsilon_{mf}$ .	Assumption of the K-L model [12].
Velocities of solids and gas in wake	Equal to upward velocity of bubble phase	Assumption of the K-L model [12].
Sparge plate	Sparge plate assumed porous	Reasonable decision based upon Hsu pilot model of fluidised bed for polysilicon production [13].
Concentration on seed particle surface	Equal to concentration in the bubble phase	Required given lack of experimental findings
Surface reaction rate limiting	In the kinetic model by Jensen, the rate of the surface reaction is limiting.	Assumption based on literature [14].
Reactor temperature	Estimated at 650°C	Value quoted widely in literature [4], [5], [13].
Reactor pressure	Maintained at 10 bar	Value quoted widely in literature [4], [5], [13].
Monosilane mole fraction	Monosilane entering the column in fluidising gas at 0.05 mole fraction	Value quoted widely in literature [4], [5], [13].

Yates notes limitations with assumptions stated, due to obvious deviation in practical usage of fluidised beds though notes that these limitations are not of significant influence to the operation of the model [12]. A diagram from Yates demonstrates assumptions in a figure below.

Figure 2: K-L model diagram from Yates, *Fluidized Bed Reactors: Processes and Operating Conditions* [12].



The proposed novel method for the fluidised bed in this volume is the sequential epitaxial growth across a set of 8 reactors. The particle size across each set of reactors will increase from 100 microns to 1000 microns incrementally and a more tailored, optimised set of reactor conditions will allow for better behaviour of the particles in fluidisation at each stage of the growth.

### 3.2. Design summary

To begin, a sample number of columns were evaluated using a simplistic calculation based upon minimum fluidisation velocity to evaluate the dimensions of reactor and required quantities. Utilising the mass flow into the column in the vapour phase, the associated volumetric flowrate could be paired with required minimum fluidisation and corresponding operational fluidisation velocity for a given particle size to provide an estimate of the reactor diameter. The particle size was increased in stages from 100 microns to 1000 microns across a sequence of 8 reactors, with the maximum permissible reactor diameter of 5 m due to the consideration of a quartz lining to inhibit homogenous deposition [5]. The resulting number of reactors was found to be 56 operating across 7 sets of 8 sequential reactors, with diameter 5 m and an aspect ratio of 1.

Firstly, various fluidisation parameters were established. All symbols are defined in the Nomenclature list. The porosity at minimum fluidisation was calculated using equation 1.

$$0.021 \frac{\mu}{\rho g} = 0.586 \Psi^{-0.72} \left( \frac{\rho_p}{\rho_g} \eta d_3 \right) \quad (1)$$

Where  $\eta = g(\rho_c - \rho_g)$ .

Equation 1: Porosity at minimum fluidisation

The minimum fluidisation was then found using equation 2.

$$u_{mf} = \frac{(\Psi d_p)^2}{150\mu} \eta \left( \frac{m_f^3}{1 - m_f} \right)$$

Equation 2: Minimum fluidisation velocity

The Reynolds number was calculated to ensure it was within the permissible range for utilisation of equation 3.

$$Re_p = \frac{\rho_g d_p U}{\mu}$$

Equation 3: Reynolds number

Particle terminal velocity was then calculated to evaluate a suitable range for operational velocity.

$$u_t = \frac{\eta d_p^2}{18\mu}, \quad Re < 0.4$$

$$u_t = \left( \frac{1.78 \times 10^{-2} \eta^2}{\rho_g \mu} \right)^{\frac{1}{3}} (d_p), \quad 0.4 < Re < 500$$

Equation 4: Maximum velocity of particle through the bed

The minimum slugging velocity was calculated.

$$u_{ms} = u_{mf} + 0.07(gD_t)^{\frac{1}{2}}$$

Equation 5: Minimum slugging velocity

The operational velocity was taken as 5 times the minimum fluidisation velocity [11] and validated to be within permissible range.

$$u_o = 5u_{mf}$$

$$u_{mf} < u_o < u_t$$

$$u_{mf} < u_o < u_{ms}$$

Equation 6: Operational velocity and permissible range

Following the initial fluidisation calculations, the K-L method from Yates could be utilised to predict behaviour in each bed. An assumption of the K-L model is noted in equation 7, with the velocity of the gas in emulsion phase adjusted for the velocity of the solids and the superficial velocity through the bed.

$$u_e = \frac{u_{mf}}{m_f} - u_s$$

Equation 7: Assumption of the K-L model

The maximum bubble diameter was then calculated.

$$d_{bm} = 0.652 (A_c(u_0 - u_{mf}))^{0.4}$$

*Equation 8: Maximum bubble diameter*

It was assumed that a porous sparge plate was utilised, as such the initial bubble diameter at the distribution plate is given by equation 9.

$$d_{b0} = 0.00376(u_0 - u_{mf})^2$$

*Equation 9: Initial bubble diameter*

The bubble diameter was found using the following equation.

$$\frac{d_{bm} - d_{b0}}{d_{bm} - d_{b0}} = e^{-0.3(D^{1/4} t)}$$

*Equation 10: Bubble diameter*

The velocity of the bubble rising in the column was then evaluated.

$$u_b = u_0 - u_{mf} + u_{br}$$

Where single bubble velocity is  $u_{br} = 0.71(gd_b)^{1/2}$

*Equation 11: Bubble rise velocity*

The volume fraction of bubbles in the bed during normal operation could then be found.

$$\delta = \frac{u_0 - u_{mf}}{u_b - u_{mf}(1 + \alpha)}$$

*Equation 12: Volume fraction of bubbles*

Where the bubble wake parameter taken as  $\alpha = 0.4$ .

The velocity of the solids was then evaluated.

$$u_s = \frac{\alpha \delta u_b}{1 - \delta - \alpha \delta}$$

*Equation 13: Velocity of solids*

The velocity of the gas in the emulsion was also evaluated.

$$u_e = \frac{u_{mf}}{m_f} - u_s$$

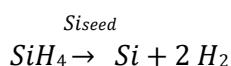
*Equation 14: Velocity of the emulsion phase*

The results of the above equations are tabulated in appendix A.



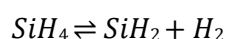
The K-L model goes on to model the rate of reaction based upon a catalytic partition coefficients, which do not apply to the pyrolysis of silane onto seed particles. Instead, the skeletal structure of the K-L model was followed, with applicable adaptations made with reference to literature where appropriate.

The governing equation for the reaction of the chemical vapour deposition of monosilane in the fluidised bed reactor is shown in equation 15 below. It typically occurs at 650 °C and 10 bar.

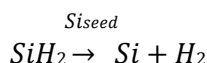


Equation 15: Governing mechanism for the pyrolysis of silane

There are various stages for the heterogeneous deposition of monosilane, though the kinetics of the general process are not well understood [14]. Jensen hypothesised that the monosilane decomposes in the gas phase to SiH<sub>2</sub>, shown in equation 16. The SiH<sub>2</sub> adsorbs onto the solidphase silicon seed particle surface, and diffuses onto a reaction site, allowing decomposition with the formation of hydrogen gas, leading to epitaxial growth of the seed particle, shown in equation 3.



Equation 16: Intermediate stage 1 in silane pyrolysis



Equation 17: Intermediate stage 2 in silane pyrolysis

The key thermochemical properties were derived from first principles, as shown in the V1 submission and are tabulated in table 8.

Table 9: Key values calculated for reaction of silane to produce polysilicon.

Key calculated values	Unit	Value
H <sub>rxn</sub> [298K]	kJ/mol	-34.31
C <sub>p,rxn</sub> [923] <sup>o</sup>	J/molK	5.46
C <sub>p,rxn</sub> [298] <sup>o</sup>	J/molK	34.85
H <sub>rxn</sub> [923]	kJ/mol	-21.71
G <sub>rxn</sub> [298] <sup>o</sup>	kJ/mol	-56.81
G <sub>rxn</sub> [923] <sup>o</sup>	kJ/mol	-112.67
lnK <sub>[298]</sub>	-	22.93
lnK <sub>[923]</sub>	-	14.68
K <sub>[923]</sub>	-	2377231.47

The large equilibrium constant and negative Gibbs free energy ensured that the process was feasible and ensured a conversion reaction could be considered rather than a more complex equilibrium ensuring greater conversion and linear epitaxial growth.

Hashimoto et al. developed a kinetic model demonstrating the Arrhenius plots with detail into development of a model to describe the pyrolysis of silane for growth of polysilicon and their results are shown below. Hashimoto quotes the rate of silicon growth as

$$r_G = \frac{2.44 \times 10^{16} \exp(-55300/T)}{1 + 8.52 \times 10^{16} \exp(-44500/T) C_{HS} C_{AS}} \quad [15].$$

Equation 18: Rate equation for growth of polysilicon

Where  $r_G$  is the rate of growth,  $C_{AS}$  is the concentration of silane on the substrate surface and  $C_{HS}$  is the concentration of hydrogen on the substrate surface.

Hashimoto also found the rate constant.

$$k = 2.03 \times 10^{21} \exp(-55300/T) \quad [15].$$

Equation 19: Rate constant for growth of polysilicon

Given an assumption that the concentration of both silane and hydrogen are the same on the catalyst surface as they are in the vapour phase at the inlet of the reactor we can evaluate the rate parameters. Given the assumption that the surface reaction is rate limiting, as found by Jensen [14], the rate parameters could be evaluated at the reactor operating conditions.

Table 10: Kinetic parameters evaluated from Hashimoto [15].

Parameter	Quantity	Units
$k_{923}$	$1.93851 \times 10^{-5}$	m/s
$k_{1066}$	0.061185	m/s
$r_G$	$1.16491 \times 10^{-11}$	mol/m <sup>2</sup> s

The K-L method could then be completed. The conversion in the reactor could be found, assuming the process is first order as reinforced by literature [14], [15] and that the fluidised bed behaves as a plug flow reactor in respect to rate profile.

$$V = - \frac{v_o}{k} \ln(1 - X)$$

Equation 20: Design equation of a plug flow reactor

Therefore, conversion could be found for the reactor by equation 22, and is tabulated below.

$$X = 1 - \exp(-\frac{hk}{u_o})$$

Equation 21: Conversion in the fluidised bed reactor

Tables 10 and 11 show the conversion, operational fluidisation velocity and corresponding deposited mass of polysilicon at temperatures of 650°C and 793.4°C respectively.

Table 11: Conversion in the fluidised bed reactor at 650°C.

$d_p$	$u_0$	Conversion	moles reacted	mass deposited
m	m/s		mol/s	g/s
0.0001	0.0657	0.001474	7.34E-05	0.002062
0.0002125	0.2291	0.000423	7.35E-05	0.002063
0.000325	0.4648	0.000209	7.35E-05	0.002064
0.0004375	0.7633	0.000127	7.35E-05	0.002064
0.00055	1.1190	0.000087	7.35E-05	0.002064
0.0006625	1.5280	0.000063	7.35E-05	0.002064
0.000775	1.9873	0.000049	7.35E-05	0.002064
0.0008875	2.4944	0.000039	7.35E-05	0.002064

The sum of the mass deposited for a single set of sequential columns is 0.01650 g/s, and across the 7 sets of these sequential columns, the mass deposited of silicon is therefore 0.4160 kg/hr.

Given the low conversion at 650°C, the reactor temperature was found for which sufficient deposition would occur to ensure nameplate capacity of the plant was met, and this was achieved utilising Excel's Goal-Seek function. The temperature at which the sufficient capacity of 980 kg/hr was reached was 1066K. The conversion data and K-L method parameters are tabulated below.

Table 12: Conversion in the fluidised bed reactor at 793.4°C.

$d_p$	$u_0$	Conversion	moles reacted	mass deposited
m	m/s		mol/s	g/s
0.0001	0.0657	0.990502	0.0493	1.386
0.0002125	0.2291	0.736921	0.1280	3.595
0.000325	0.4648	0.482234	0.1699	4.772
0.0004375	0.7633	0.330214	0.1911	5.367
0.00055	1.1190	0.239200	0.2030	5.699
0.0006625	1.5280	0.181441	0.2102	5.903
0.000775	1.9873	0.142677	0.2150	6.037
0.0008875	2.4944	0.115420	0.2183	6.130

The sum of the mass deposited for a single set of sequential columns is 38.887 g/s, and across the 7 sets of these sequential columns, the mass deposited of silicon is therefore 979.99 kg/hr.

### 3.3. Implications of shortcut design

The various assumptions associated with K-L model were made and as discussed should not affect reasonable performance of the reactor. However, the assumptions made to appropriate Hashimoto's rate model into the K-L method gives reason to question the accuracy of the shortcut design. The concentration of the reactant, monosilane, in the gas phase at the base of the column is likely to be quite different to the concentration of the  $\text{SiH}_2$  on the silicon seed particle surface, especially given the assumption of the reactor behaving as a plug flow reactor in terms of rate behaviour, thus causing a contradiction in the model since the PFR rate profile dictates a constant rate profile along the reactor and thus consumption of the monosilane leading to decreasing concentrations of reactant at increasing length along the reactor.

The shortcut design does not account for side reactions and despite the literature consultation to ensure optimal reactor conditions were selected, there would be a tendency for the monosilane to form longer chain silane compounds such as  $\text{Si}_2\text{H}_6$ ,  $\text{Si}_3\text{H}_8$  etc. as investigated by Frenkach [16]. Despite the extent of such side reactions being minimal, over the course of annual operation of such a large capacity plant, the undesirable side reaction would account for a significant loss across the plant which the shortcut does not account for.

Given the assumptions on operational temperature and pressure, as found from the literature survey conducted, the operating conditions of the reactor are very consistent amongst all sources as they must satisfy the condition of sufficient temperature to allow for monosilane pyrolysis and the pressure aids kinetics [4], [13]–[15]. As such, these are taken as constant parameters and the reactor design is highly dependent on these operating conditions. The behaviour outside specified conditions with regards to side reactions and fines formation is unknown.

### 3.4. Alternative arrangements

Alternative arrangements for the reactor system are relatively limited outwith manipulation of reactor dimensions, sequential setup and overall quantity. There are strict constraints on feed and product requirements which do not allow for leeway in selection of the arrangement of the reactors, given operation is dependent on sufficient fluidisation in the reactors.

The main alternative which would considerably reduce CAPEX costs of the plant but would increase selectivity of the homogeneous deposition of monosilane is increasing the molar ratio of the monosilane to hydrogen in the feed gas. Hydrogen acts against Le Chatelier's principle in monosilane pyrolysis but enhances the desirable heterogeneous deposition of the silicon. Without hydrogen, significant increase in fines formation is observed [5], [17]. Manipulation of the molar ratio at the inlet of the reactor could allow for significantly fewer reactors required, though based upon empirical data would significantly increase undesirable products. Due to the proprietary nature of the ongoing R&D into fluidised bed reactors, there is a lack of data on the outcome of such experimental findings, and as such, the quantity of fines production at increased monosilane concentrations is unknown. The throughput of the reactors would also increase twofold if found feasible to not use fluidising hydrogen gas, but relevant cost-benefit analysis should be performed when such data becomes available. There was no employment of computational model due to the infeasibility and multifaceted nature of CFD modelling in applicability to a complex, unknown kinetic model.

## 4. Operation of equipment and control, Start-up & Shutdown

### 4.1. Description of normal operation, start-up and shutdown

#### 4.1.1. Commissioning and Pre-Commissioning

Before the start-up procedure for the process can commence, some steps need to be taken to ensure that it will run smoothly and safely. Pre-commissioning and commissioning are the

first of these steps, and consideration for pre-commissioning and commissioning phases are given in detail in the V1 submission.

#### 4.1.2. Start-up

The process for the start-up procedure of the fluidised bed reactor is relatively simple. The primary objective to ensure sufficient operation is for the temperature of the reactor to reach operational level of 793°C. The start-up sequence of the reactor along with auxiliary equipment is detailed table 10 in appendix B. The location of the fluidised bed at the end of the process and without the need to develop significantly sized recycle streams allows for a relatively simple start-up process. Once sufficient production of monosilane is occurring in V1 plant area 40, the operation of the fluidised bed can begin, with the time to reach fluidisation rapid the main constraint is reaching sufficient temperature which can be assisted by initial increase of the heating duty across the reactor jacket. The traditional start-up procedure for fluidised beds of burning catalyst is not feasible given the associated risk release of environmentallydamaging chlorosilane compounds which could exist as trace compounds in the reactor during the start-up procedure.

##### 4.1.2.1. *Time to Steady State*

The time to reach steady state for the fluidised bed is based on the sequence of start-up. The fluidised bed is the final area of the plant in the start-up procedure, given the individual startup time of 42 minutes per reactor and assuming the worst case scenario of individual start-up of each reactor in sequence simultaneous to other reactors located in the same position of another sequence, the total time to steady state would be 4.9 hours. It is assumed that previous to this 4.9 hour period of time to reach steady state operation that auxiliary units including turbomachinery and heat exchangers were given sufficient time to reach normal operation at the same time as the fluidised bed reactors. The total plant time to steady state is provided in V1 submission as 17.3 hours neglecting accumulation of recycle streams, so a conservative estimate of 24 hours is given, as such the start-up of fluidised bed reactors would occur in the final 6 hours of start-up of the whole plant. The details of each unit and respective time to steady state is detailed in table 12 in appendix B.

#### 4.1.3. Normal Operation

The normal operation of the fluidised bed reactor is accurately represented by the PFD description, though the description does not account for the cycling of reactors or the simultaneous operation of the reactors in sequence. The reactors are cycled to ensure sufficient time for the maintenance process whilst maintaining production volume. Therefore, when designing the plant 72 reactors were considered for the required number of reactors, due to the normal operation of 7 sets of 8 reactors in sequence, with an additional two sets of 8 in scheduled maintenance. Sinnott details the maintenance process of such a plant, and the downtime for reactors would allow for performance checks of auxiliary heat exchangers and coolers to be evaluated, along with the cleaning of silicon fines deposited on the reactor [18]. The time between scheduled maintenance should be monitored based upon performance of the reactor and once deviation optimal reactor conditions occurs, maintenance should occur.

#### 4.1.4. Shut Down

The process for the shutdown procedure of the fluidised bed reactor is also relatively simple. The cooling of the reaction vessel must begin by reducing the flow of seed particles into the reactor, before reducing the flowrate of the fluidising gas. Monosilane feed should be stopped before the feed of hydrogen to halt the reaction, and slow reduction of the flow of hydrogen can allow for de-fluidisation of the bed back to a fixed bed state. The full sequence for the shutdown of the process and auxiliary units is detailed in table 11 of Appendix B. Efforts should be made to ensure purging of the system using nitrogen responsibly disposes of the vent

gases of the process, as release of monosilane to surrounding air can result in auto ignition of the monosilane.

#### 4.1.4.1. *Emergency Process Shut Down*

The emergency shut-down of the reactor should be an infrequent process, however the necessary precautions and procedures must be detailed for efficient care and safety of the workers, the wider plant and surrounding environment.

Manual shutdown of the milling area should occur, to pre-empt the automatic stop to sequester the risk of dust explosions. The roller crusher and ball mills must be shut down separately, and all the shutdown operations should be carried out locally or from the control room. When all equipment is shut down, the cyanide metering pump and lime timer should be switched off and all shut-off valves closed in the air and solution lines [19]. To reduce the impact of turbomachinery failure on the rest of the process, backups should be installed with along with isolation and bypass pipework.

The use of hydrogen and monosilane in a fluidised bed reactor poses a potentially significant safety risk and should be treated accordingly in any operation. Both of the components can form explosive mixtures when combined with air; in fact, monosilane is spontaneously combustible in air [20]. As a result, any leaks or pipe failure may result in fire or explosion. This risk is only amplified by the elevated temperature of the FBR in the silicon production process. It is therefore vital that effective measures are put in place to execute an emergency shutdown to prevent accident. The operation of an FBR should be shut down immediately if any one of the following 10 abnormalities is detected:

1. **High temperature:** Prevents thermal damage to the reactor and catalyst deterioration.
2. **Low temperature:** Prevents the formation of explosive gas mixtures resulting from the increased concentration of unreacted materials (due to lower catalytic activity) as well as preventing possible downstream combustion.
3. **High pressure:** Prevents the potential destruction of the reactor due to overpressure.
4. **High oxygen concentration:** Prevents the formation of explosive gas mixtures.
5. **Low oxygen concentration:** Prevents catalyst degradation (reductive).
6. **High raw material gas concentration:** Prevents excess capacity of waste gas incinerator.
7. **High raw material gas flowrate:** Prevents catalyst degradation (reductive and thermal) and reactor thermal damage.
8. **Low raw material gas flowrate:** Prevents explosion due to gas mixture.
9. **High oxygen containing gas flowrate:** Prevents explosion due to gas mixture.
10. **Low oxygen containing gas flowrate:** Prevents catalyst degradation (reductive).

An emergency shutdown of the fluidised bed reactor constitutes the immediate shutoff of raw material feed and fluidisation gas. Any gas remaining in the reactor should be sent to flare. List adapted from Emergency shutdown of fluidized bed reaction system by Sano et al [21].

## 4.2. Control strategy

The main control loops are demonstrated on the PFD and follow traditional practice. Operation and usage should be computational, utilising suitable combinations of proportional, integral and derivative controller mechanisms. All critical control loops are shown on the PFD, and traditional practice for control of auxiliary units is implied.

### 4.2.1. Flowrate Control

A flowrate controlled is used in various areas of the system, such as on the flow on nitrogen for the milling of seed crystals of polysilicon. As shown in V1, from empirical findings, a flow of nitrogen is required based upon the quantity of polysilicon to be crushed [22]. Given this

required ratio of nitrogen per unit of polysilicon, an integrated control loop with controlled variable of flow of nitrogen and disturbance variable of the flow of polysilicon.

#### 4.2.2. Level Control

A level control is used on the flash drum used for the separation of the vent gases, where the liquid phase is monosilane for recycle. The controlled variable is the outlet flowrate of the liquid from 50-TK-002, and the manipulated variable is the liquid level of the vessel. All surge tanks and intermediate drums not shown on the PFD would employ similar control loops.

#### 4.2.3. Composition Control

The composition of the feed gas to the reactor shown as stream 94 on the PFD must contain a mole fraction of monosilane of 0.05. Thus, the composition is controlled by adjusting the flow of hydrogen corresponding to the sufficient amount to ensure accurate mole fraction of monosilane is maintained. The controlled variable is the composition of stream 94, measured variable is the flow stream 91 and the manipulated variable the flowrate of stream 92.

#### 4.2.4. Temperature Control

A simple feedback control loop is employed across all heat exchangers to ensure sufficient temperature control in the system. With manipulated variable being the flow of duty fluid, and controlled variable temperature of the flow of outlet fluid. The usage of such systems is critical to account for the range in temperature of available duty fluid across seasonal temperature ranges as well and the large amount of possible disturbance variables. Sufficient temperature control is critical for optimal reactor performance, as such the control of such variables are of extreme importance.

#### 4.2.5. Pressure Control

A pressure control loop is utilised to ensure all tanks and drums operate at required pressure. A simple feedback control loop is utilised with manipulated variable the flow of the outlet of fluid from the tank and controlled variable of the pressure in the tank. In case of overpressure, pressure relief valves are also employed on all tanks which operate above atmospheric pressure, with a flare or purge system to waste disposal utilised.

### 4.3. Safety systems & Fugitive emissions

Pressure relief valves are utilised as discussed above and exist as the primary safety system in case of overpressure. Emergency shutdown procedure, also detailed previously, can result in the requirement to purge the system and thus there exists significant risk to the workers and surrounding environment. Despite the tendency of monosilane to explode in air with limited oxygen content, auto ignition of monosilane is observed at low temperatures under dynamic equilibrium between temperature and oxygen concentration. There is no risk for the leaking of hydrogen, nitrogen or polysilicon, with nitrogen and hydrogen both abundant in the air already, and polysilicon in solid state has limited safety considerations. The opportunity to reduce the explosivity of monosilane can be achieved by the addition of inhibitor methyl iodide, but this comes at a financial cost [23]. Full details of safety procedures and environmental hazards for all substances is detailed in the V1 submission, but the main safety procedures detailed include intensification, substitution, attenuation, limitation of effect, simplification and containment [24]. Another primary concern with respect to the fluidised bed reactor is utilisation of hydrogen gas as a safety mitigation to reduce the quantity of silicon fines and thus reduce the associated risk of dust explosion. Pneumatic transport is used to transport dust to mitigate the risk of explosion.

As a fugitive emission, monosilane causes no ecological damage on release to the environment, but can form acid gases during combustion and release should be avoided. Further detail is given in the V1 submission.





## 5. Critical Review of Design

### 5.1. Shortcut design performance

The design in section 3 specified at 650°C clearly does not meet the required specifications for conversion of monosilane, with only 0.04% of the required 980 kg/hr of polysilicon production being produced, thus not meeting the nameplate capacity of the plant of 7840 T/yr. At the operating conditions of 793°C and 10 bar, the nameplate capacity of the plant is met and sufficient design that meets the required specifications obtained. The V1 was centred around an assumption of conversion of 80% based on literature values [25] and an operational temperature of 650°C, but this was found to be too low and instead must be increased to 793°C with minimal other changes required.

If the suggested change to operational temperature is not feasible due to safety considerations, then the design becomes infeasible. Given the suggested temperature increase to 1066K is less than 1200K explored extensively in literature, the suggested operating temperature seems feasible [15]. There is difficulty in alternate solutions to rectify design if temperature alteration is not feasible, including manipulation of the column setup. Given the dependency and iterative nature of the K-L method, perhaps the easiest solution is to increase the column aspect ratio from 1 to a significantly larger ratio of around 5, though this influences various parameters evaluated throughout and would lead to extremely tall, expensive reactors. The difficulty associated with the unsuitable design at 650°C include the subsequent recycle of unreacted monosilane of increased flowrate than initially estimated, and again, an iterative process to evaluate the steady-state of the system is required. The capacity being met and specified at an increased temperature seems a reasonable finding of the shortcut design and given the reasonable assumptions associated with the K-L method, the author suggests that operation of a fluidised bed reactor for the pyrolysis of monosilane via CVD to form polysilicon is a feasible, operable procedure.

Given assumptions of the K-L method, the general performance of the reactor is sufficient and the mass transfer between bubble and emulsion phase understood. Perhaps the most significant limitation in the design is the lack of understanding in the heat transfer behaviour of the model, which is discussed in section 5.3.

### 5.2. Operability beyond flowsheet specifications

The shortcut model developed has limited range when exceeding flowsheet specifications. The K-L model does not allow for a broad understanding of the system beyond mass transfer between bubble and emulsion phases, which in itself holds a temperature dependency with respect to reaction kinetics and rate. Under normal operating conditions, the model performs well, but beyond specified conditions such as under different fluidisation regimes like slugging or a fixed bed state completely changes the assumptions made during the K-L method and thus hinders the ability to account for the behaviour in the system. Behaviour of the reactor during periods of slugging is unsafe, and during fixed bed states is non-optimal, which makes prediction of such regimes difficult. The sensitivity analysis in section 5.4 demonstrates the temperature dependence of the system.

Significant bottlenecking in the process occurs due to low conversion of monosilane requiring large flowrates of monosilane for a sufficient deposition of polysilicon – the shortcut model developed cannot solve this behaviour but the author recognises the dependency of the system on an inherent, albeit minor flaw. The turndown of the system occurs at the minimum permissible velocity to ensure suitable fluidisation in the system and is shown in the K-L method. The reverse for maximum velocity through the column,  $u_t$ , is also shown in the K-L method, though slugging may occur before maximum gas velocity is reached.

### 5.3. Limitations of shortcut design

Perhaps the largest neglected factor in the shortcut design is the neglect for the heat transfer between bubble, cloud and emulsion phases. This heat transfer would influence rate behaviour due to the exothermic nature of the process, and holds the possibility of thermal runaway if not accounted for. Given the fluidisation gas enters the reactor at 300°C, the heating duty required to maintain the reactor temperature is an important variable for normal operation and the K-L method does not account for this. A suitable shortcut calculation can be performed utilising K-L method of a different form and requires data on heat transfer coefficients between the solid and gas phase which were not available.

The heat is also neglected across the reactor and does not account for the temperature profile across the reactor jacket, given the silica lining – it would be expected to act as insulating but must be of a radius greater than the critical radius of insulation to do so. As such, duty for heating of the reactor during normal operation must account for losses to the surrounding environment as well as the exothermic reaction.

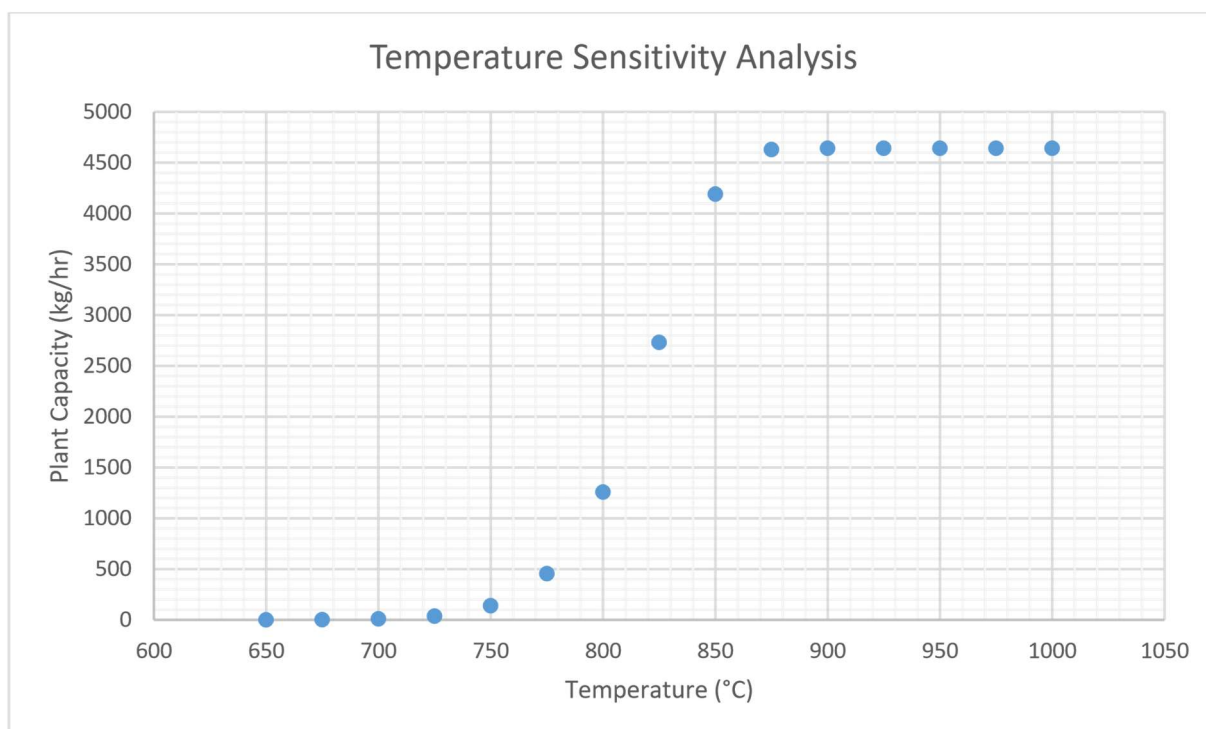
As previously discussed, the assumptions of the K-L method are well understood and Yates describes there are obvious deviation in practical usage of fluidised beds though notes that these limitations are not of significant influence to the operation of the model [12].

Another significant omission from the shortcut is the accounting of side reactions. There are various possible side reactions via different intermediates and pathways for the pyrolysis of monosilane, though the major ones include homogeneous deposition of polysilicon forming fines, or the formation of long chain silane molecules such as  $\text{Si}_2\text{H}_6$ ,  $\text{Si}_3\text{H}_8$  etc. The K-L method does not account for the extent or selectivity of side reactions, though effort was made to account for these omissions in literature survey when obtaining optimal reactor conditions [4], [13], [16], [17]. Literature suggests the primary approach for minimisation of fines formation occurs by manipulation of fluidisation conditions, with mole fraction of monosilane in a fluidising gas of differing composition the manipulated variables [25]. The consideration for the fluidisation gas utilised for the fluidised bed was considered with reference to various literature sources [4]. Options exist including hydrogen, nitrogen, argon or other inerts; and despite the apparent inhibition exhibited by hydrogen due to Le Chatelier's principles, literature sources evaluate hydrogen in particular due to the minimisation of the selectivity to the homogeneous deposition of monosilane onto undesirable fine particles, which currently possess no additional value and demonstrate a waste of feed. Nitrogen and argon appear to increase the selectivity to the homogeneous deposition, increasing production of financially futile product so were not considered for the final design. With regards to the selectivity to longer chain silanes, due to a lack of understanding of the kinetics of monosilane pyrolysis, development of a sufficient model to account for a large quantity of side reactions was not feasible in a shortcut design.

### 5.4. Sensitivity of shortcut design

A sensitivity analysis of the design to the temperature in the reactor and associated dependency on rate was performed and the method for the conversion was the same as followed in section 3.2 but at differing temperatures with corresponding rate constants. The results are graphed below, though they neglect the impact of increased temperature on influences of monosilane auto ignition or pyrolysis, as well as selectivity to the primary side reaction that is homogenous deposition. Despite the obvious benefit of increased reactor temperature, the associated safety considerations for operation at high temperature leads to the optimal temperature operation at 793.4°C.

*Figure 3: Sensitivity Analysis on the Temperature dependence of rate*



A sensitivity analysis was not feasible for the increase in particle size given the inherent requirement in the development of the fluidisation parameters for the K-L method. For varying flowrates of fluidisation gas, the behaviour trends linearly with flowrate due to the parameters developed in the K-L method. Pressure is not accounted for in the rate equations as such could not be accounted for in a sensitivity analysis. An improvement on the availability of data on the influence of the molar fraction of monosilane at the inlet of the reactor would add significantly to the design and allow for suitable optimisation of the fluidisation gas to reduce fines formation whilst also ensuring maximum possible deposition of polysilicon for rapid epitaxial growth.

### 5.5. Accurate methods for design

If tasked with designing the reactor given unlimited time and resource, I would recommend a full computational model developed utilising the Hsu et al. reactor setup [13] modelled using CAD software, and then inputted into CFD software such as STAR-CCM+ with consideration of the rate behaviour developed by Hashimoto. The main limitations on behaviour understanding of the plant is inherently linked to the confusion of behaviour of turbulent regimes during scale up. This is the main limitation in the polysilicon industry and inherently linked to the solving of the Navier-Stokes Equations Millennium Problem, or simply a welldefined empirical model.

For more practicable solutions which would benefit the shortcut design, the development of a kinetic model which fits the traditional K-L method without adaptation would allow for the model to be utilised as intended utilising the catalyst parameters,  $\gamma$  [12]. For such a model to be established, more accurate understanding of the kinetics of monosilane pyrolysis is required, as well as diffusion rates between bubble, emulsion and cloud phases established.

It would be important to develop an understanding of monosilane behaviour across a range of inlet concentrations to allow for optimisation of feed concentration and allow for a detailed understanding of rate profile through the reactor rather than the idealised assumption plugflow.

Also of great significance would be understanding of the heat transfer in the bed and allow the design to fulfil the requirement for the understanding of reactor temperature profiles and required duty for maintenance of optimal reactor conditions.

## 5.6. Group dynamic and characteristics

Throughout the time spent working on DP4, especially considering the circumstances under which we were required to interact, I had a very positive experience with my group. It was decided very early on that the group would split and work in two halves, one focussed on the design of the Siemens plant with a TCS feed and the other half designing the FBR plant. As such, I interacted more frequently with those working on the FBR plant and believe we all worked coherently and our personalities were well suited. The group dynamic amongst the FBR group was assisted by everyone being focussed, dedicated and hard-working and our group work styles complimenting one another. There was no obvious chairperson or leader if we were to quote Belbin team roles, but as an implementer myself, I was happy to take a leadership role within the FBR group when required, maintaining communication between the two groups and ensuring schedules were kept to. We had a well-developed plan and established how to split the workload regarding who was responsible for each section, where I took responsibility for thermodynamics and thermochemistry, the PFD collation and contributed as to a group effort on the mass and energy balances, as well as introduction and conclusion. I would like to praise Kai's efforts of start-up and shutdown sections, Charlegne and John's combined efforts on economics and collation of mass and energy balances, and finally Peter's efforts on safety and environmental considerations, but more than anything – the whole groups cohesion as one. Extra praise must be given to John and his due-diligence with dedication to well formatted Excel spreadsheets, given the finding of an error with two days before submission leading to the re-evaluation of the whole economics section due to a minor error in the mass balances leading to a 25% overproduction in the plant. Without such care in the spreadsheets when initially conducting these calculations, rectification of this error would have been impossible, though it did lead to a full night of work before the submission – I am pleased we were able to fix it. There were no instances of non-attendance and effort was made on behalf of everyone to ensure completion to a high standard. As far as I worked with the Siemens group, I also had a very positive experience and they held themselves to a very high standard – always sure to complete work on time, albeit sometimes needing to redo once someone in the FBR group had checked the work, this was never a sticking point. I would also like to praise both group supervisors I worked with, firstly Santiago for accurate and insightful direction when I was researching to specific texts and help on UNISIM software when it proved to be a significant struggle. Secondly, to Carlos who was vital for the group during the 2 week period of high stress before the final submission.

## 6. References

- [1] PV- TECH, "Polysilicon consumption to decline below 4g/W in Q3 2018." .
- [2] G. Gatticchi and M. Vanek, "South Africa's Cities to Switch to Solar as Power Monopoly Ends," 2020. .
- [3] "Chapter 1 - Introduction," in *Chemical Process Equipment: Selection and Design*, 2nd ed., 2005, pp. 1–16.
- [4] R. Lutwack, "Proceedings of the Flate-Plate Solar Array Project Workshop on Low-Cost Polysilicon for Terrestrial Photovoltaic Solar-Cell Applications Proceedings of the

- Flate-Plate Solar Array Project Workshop on Low-Cost Polysilicon for Terrestrial Photovoltaic Solar.”
- [5] W. O. Filtvedt *et al.*, “Development of fluidized bed reactors for silicon production,” *Sol. Energy Mater. Sol. Cells*, vol. 94, no. 12, pp. 1980–1995, 2010, doi: 10.1016/j.solmat.2010.07.027.
  - [6] M. E. Materials and S. Peters, “Polysilicon Materials FBR Technology for Solar and Semiconductor Silicon Graham R. Fisher and Milind Kulkarni MEMC Electronic Materials, Inc., St. Peters, MO63376, U.S.A.,” vol. 27, no. 1, pp. 1001–1006, 2010.
  - [7] J. Bernreuter, “Technology Review Fluidized Bed Reactor 2020.,” *BERNREUTER Res.*, 2020.
  - [8] D. Yang, *Handbook of photovoltaic silicon*. 2019.
  - [9] L. Jiang, B. F. Fieselmann, L. Chen, and D. Mixon, *Handbook of Photovoltaic Silicon*. 2017.
  - [10] D. Kunii and O. Levenspiel, “The K-L reactor model for circulating fluidized beds,” *Chem. Eng. Sci.*, vol. 55, no. 20, pp. 4563–4570, 2000, doi: 10.1016/S00092509(00)00073-7.
  - [11] D. Kunii and O. Levenspiel, *Fluidization Engineering*, 2nd ed. 1991.
  - [12] J. G. YATES, “Fluidized Bed Reactors: Processes and Operating Conditions,” vol. 168, no. (NOVEMBER, 1975), pp. 1–44, 1975, doi: 10.1021/bk-1983-0226.ch003.
  - [13] G. Hsu, N. Rohatgi, and J. Houseman, “Silicon particle growth in a fluidized- bed reactor,” *AIChE J.*, vol. 33, no. 5, pp. 784–791, 1987, doi: 10.1002/aic.690330511.
  - [14] K. F. Jensen and D. B. Graves, “Modeling and Analysis of Low Pressure CVD Reactors,” *J. Electrochem. Soc.*, vol. 130, no. 9, pp. 1950–1957, 1983, doi: 10.1149/1.2120129.
  - [15] K. Hashimoto, K. Miura, T. Masuda, M. Toma, H. Sawai, and M. Kawase, “Growth Kinetics of Polycrystalline Silicon from Silane by Thermal Chemical Vapor Deposition Method,” *J. Electrochem. Soc.*, vol. 137, no. 3, pp. 1000–1007, 1990, doi: 10.1149/1.2086544.
  - [16] M. Frenklach, L. Ting, H. Wang, and M. J. Rabinowitz, “Silicon particle formation in pyrolysis of silane and disilane,” *Isr. J. Chem.*, vol. 36, no. 3, pp. 293–303, 1996, doi: 10.1002/ijch.199600041.
  - [17] W. O. Filtvedt, T. Mongstad, A. Holt, M. Melaaen, and H. Klette, “Production of silicon from SiH<sub>4</sub> in a fluidized bed, operation and results,” *Int. J. Chem. React. Eng.*, vol. 11, no. 1, pp. 57–68, 2013, doi: 10.1515/ijcre-2012-0027.
  - [18] G. Towler and R. Sinnott, *Chemical Engineering Design. Principles, practice and economics of plant and process design*. 2008.
  - [19] L. D. Michaud, “Ball Mill Operation -Grinding Circuit Startup & Shutdown Procedure,” *911Metallurgist*, Feb. 2016. .
  - [20] L. Jiang, B. F. Fieselmann, L. Chen, and D. Mixon, “Fluidized bed process with silane,” in *Handbook of Photovoltaic Silicon*, Springer Berlin Heidelberg, 2019, pp. 69–108.

- [21] K. Sano, Y. Koshiba, and H. Ohtani, "Emergency shutdown of fluidized bed reaction systems," *J. Loss Prev. Process Ind.*, vol. 68, no. August 2019, p. 104277, 2020, doi: 10.1016/j.jlp.2020.104277.
- [22] R. MacDonald, "Optimisation and Modelling of the Spiral Jet Mill," no. February, p. 196, 2017.
- [23] A. N. Baratov, "EXPLOSIVITY OF MONOSILANE-Air MiXTURES," vol. 407, no. I, pp. 407–408, 1967.
- [24] A. Heikkil, "Inherent safety in process plant design, Technical research center of Finland," pp. 1–132, 1999.
- [25] M. P. Tejero-Ezpeleta, S. Buchholz, and L. Mleczko, "Optimization of reaction conditions in a fluidized-bed for silane pyrolysis," *Can. J. Chem. Eng.*, vol. 82, no. 3, pp. 520–529, 2004, doi: 10.1002/cjce.5450820313.
- [26] "Centrifugal Pump Start-up Procedure - EnggCyclopedia," *EnggCyclopedia*, Oct. 2011.
- [27] K. Toprak, "Startup and loading," *COURSE 234 - TURBINE Aux.*

## 7. Appendices

### Appendix A – Shortcut Calculation

Full parameters evaluated for operating temperatures of 650°C and 793°C are shown in tables 14 and 15 below.

Table 13: Shortcut design utilising K-L Method at 650°C

$d_p$	$\epsilon_{mf}$	$u_{mf}$	Re	$u_t$	$u_{ms}$	$u_0$	$d_{bm}$	$d_{b0}$	$d_b$	$u_{br}$	$u_b$	$\delta$	$u_s$	$u_e$
m		m/s		m/s	m/s	m/s	m	m	m	m/s	m/s		m/s	m/s
1.00E-04	0.493779312	0.016642	0.052954	0.67806	4.919141	0.083210208	1.822914042	0.001666177	0.473700439	1.530540218	1.597108385	0.04229747	0.028722	0.004981
0.0002125	0.462437093	0.058129	0.393047	1.999689	4.960629	0.290646029	3.00636221	0.020328091	0.794253727	1.981857768	2.214374591	0.10900962	0.113945	0.011757
0.000325	0.445655261	0.118014	1.22041	3.058348	5.020513	0.590067553	3.990765786	0.083785967	1.096403948	2.328510217	2.800564259	0.17912417	0.267822	-0.003013
0.0004375	0.43427797	0.193912	2.699437	4.117006	5.096411	0.969559018	4.867716165	0.226212354	1.429205571	2.658521657	3.434168872	0.24524903	0.513043	-0.066528
0.00055	0.425717336	0.284388	4.97697	5.175665	5.186888	1.421940783	5.673462005	0.486553768	1.830905874	3.009025453	4.14657808	0.30347404	0.875186	-0.207165
0.0006625	0.41888009	0.388439	8.188412	6.234324	5.290939	1.942195727	6.427065772	0.907723978	2.338236805	3.400455521	4.954212103	0.35229402	1.377569	-0.450241
0.000775	0.413203167	0.505306	12.46083	7.292983	5.407805	2.526529651	7.140116638	1.536089844	2.98855148	3.844352681	5.865576402	0.39185066	2.036671	-0.813772
0.0008875	0.408359104	0.634385	17.91481	8.351642	5.536885	3.171926351	7.820324685	2.421107141	3.820485951	4.346624824	6.884165905	0.42320378	2.859681	-1.306182

Table 14: Shortcut design utilising K-L Method at 793.4°C

$d_p$	$\epsilon_{mf}$	$u_{mf}$	Re	$u_t$	$u_{ms}$	$u_0$	$d_{bm}$	$d_{b0}$	$d_b$	$u_{br}$	$u_b$	$\delta$	$u_s$	$u_e$
m		m/s		m/s	m/s	m/s	m	m	m	m/s	m/s		m/s	m/s
1.00E-04	0.500520555	0.013139	0.047128	0.75	4.915639	0.065695938	1.658482734	0.001038592	0.430617914	1.459280901	1.511837652	0.035191673	0.022384485	0.003867
0.0002125	0.468750442	0.045821	0.349249	1.583206	4.94832	0.229105094	2.733439366	0.012630988	0.717814944	1.884078963	2.067363038	0.091495023	0.086776886	0.010975
0.000325	0.451739498	0.092953	1.083574	2.421374	4.995453	0.464765996	3.627348518	0.051980028	0.978650395	2.199918745	2.571731542	0.15228262	0.199099064	0.006668
0.0004375	0.440206881	0.152658	2.395568	3.259541	5.055157	0.763289742	4.423553834	0.140199567	1.250366947	2.486632438	3.097264232	0.211764406	0.372914007	-0.026127
0.00055	0.431529374	0.223805	4.41512	4.097709	5.126304	1.119022525	5.155028588	0.301332154	1.559321832	2.776903144	3.672121164	0.266529532	0.624529135	-0.105898
0.0006625	0.424598784	0.305603	7.261971	4.935877	5.208102	1.528014989	5.839109134	0.561853445	1.929621964	3.089078675	4.311490666	0.314758823	0.970490531	-0.250745
0.000775	0.418844358	0.397456	11.04847	5.774045	5.299956	1.987281283	6.486333634	0.950356399	2.385180829	3.434420814	5.02424584	0.355840124	1.425064472	-0.476129
0.0008875	0.413934162	0.49889	15.88122	6.612213	5.401389	2.494448341	7.103712104	1.49732766	2.950400356	3.819735828	5.815294501	0.389997572	1.998179519	-0.79294





A sample calculation is provided below for the first reactor which sees the growth of polysilicon crystal from 100 to 212.5 microns. The results of the calculation are tabulated in table 12 for each respective particle size increase. Suitable dimensional analysis was performed where required, and SI units are implied unless specified otherwise.

Viscosity of gas phase and density of gas phase were taken as the weighted average of hydrogen and monosilane viscosity at 650°C. The mole fraction of hydrogen and monosilane as defined as 0.95 and 0.05 respectively correspond to mass fractions of 0.55 and 0.45 respectively, using their respective molecular weights.

$$\mu = x_{\text{hydrogen}}\mu_{\text{hydrogen}} + x_{\text{monosilane}}\mu_{\text{monosilane}} = (0.55 \times 1.79346 \times 10^{-5}) + ((1 - 0.55) \times 0.0000337) = 2.50291 \times 10^{-5} \text{ Pa.s}$$

$$\rho_g = x_{\text{hydrogen}}\rho_{\text{hydrogen}} + x_{\text{monosilane}}\rho_{\text{monosilane}} = (0.55 \times 0.558) + ((1 - 0.55) \times 1.313) = 0.89775 \text{ kg m}^{-3}$$

Firstly, various fluidisation parameters were established. The porosity at minimum fluidisation was calculated using equation 1.

$$\psi_{mf} = \frac{-0.72 (\rho_p - \rho_g) d_p}{(\rho_p - \rho_g)} = 0.586 \Psi$$

Where  $\eta = g(\rho_c - \rho_g)$ .

Equation 22: Porosity at minimum fluidisation

Using a value of sphericity of 0.86, assumed equal to silicon dioxide quoted in Fluidization Engineering [11], the viscosity and density of the gas phase, density of polysilicon of 2330 kg/m<sup>3</sup>, a particle size of 100 µm and a g value of 9.81 m/s<sup>2</sup> the porosity at minimum fluidisation could be found.

$$\psi_{mf} = \frac{-0.72}{0.586(0.86)} \frac{(0.89775 \times (9.81 \times 0.50291(2330 - 0.89775)^{-52})) \times 1 \times 10^{-43}}{(0.2330 - 0.89775)} = 0.500520555$$

The minimum fluidisation was then found using equation 2.

$$u_{mf} = \frac{(\Psi d_p)^2}{150 \mu} \eta \left( \frac{\rho_p}{1 - \psi_{mf}} \right)^3$$

Equation 23: Minimum fluidisation velocity

$$u_{mf} = 150 \frac{(0.86 \times 1 \times 10^{-4})^2}{2.50291 \times 10^{-5}} \times (9.81 \times (2330 - 0.89775)) \times (1 - 0.500520555)^3 = 0.013139188 \text{ m s}^{-1}$$

The Reynolds number was calculated to ensure it was within the permissible range for utilisation of equation 3.

$$Re_p = \frac{\rho_g d_p u_{mf}}{\mu}$$

Equation 24: Reynolds number

$$Re_p = \frac{0.89775 \times 1 \times 10^{-4} \times 0.013139188}{2.50291 \times 10^{-5}} = 0.047128059$$

Particle terminal velocity was then calculated to evaluate a suitable range for operational velocity.

$$u_t = \left( \frac{1.78 \times 10^{-2} \eta^2}{\rho_g \mu} \right)^{\frac{1}{3}} (d_p), \quad 0.4 < Re < 500$$

Equation 25: Maximum velocity of particle through the bed

$$u_t = \frac{78 \times 10^{-2} \times (9.81 \times (2330 - 0.89775))}{0.89775 \times 2.50291 \times 10^{-5}}^{\frac{1}{2}} = 0.75 \frac{m}{s}$$

The minimum slugging velocity was calculated.

$$u_{ms} = u_{mf} + 0.07(gD_t)^{\frac{1}{2}}$$

Equation 26: Minimum slugging velocity

The column diameter was taken as 5m.

$$u_{ms} = 0.013139188 + 0.07(9.81 \times 5)^{\frac{1}{2}} = 4.91563855 \frac{m}{s}$$

The operational velocity was taken as 5 times the minimum fluidisation velocity [11] and validated to be within permissible range.

$$u_o = 5u_{mf} = 0.065695938 \frac{m}{s}$$

Equation 27: Operational velocity

The maximum bubble diameter was then calculated.

$$d_{bm} = 0.652 (A_c(u_o - u_{mf}))^{0.4}$$

Equation 28: Maximum bubble diameter

Where cross sectional area was evaluated as:

$$A_c = \frac{\pi}{4} D_c^2 = 19.63495408 m^2$$

$$d_{bm} = 0.652(19.63495408 \times (0.065695938 - 0.013139188))^{0.4} = 1.658482734 m$$

It was assumed that a porous sparge plate was utilised, as such the initial bubble diameter at the distribution plate is given by equation 9.

$$d_{b0} = 0.00376(u_0 - u_{mf})$$

Equation 29: Initial bubble diameter

$$d_{b0} = 0.00376(0.065695938 - 0.013139188)^2 = 0.001038592 \text{ m}$$

The bubble diameter was found using the following equation.

$$d_{bm} - d_b = e^{-0.3(D \sqrt{h_t})}$$

$$\frac{d_{bm} - d_{b0}}{d_{bm} - d_b}$$

Equation 30: Bubble diameter

Where height was taken from the aspect ratio of 1.

$$\Rightarrow d_b = d_{bm} - (d_{bm} - d_{b0}) \times e^{-0.3(\frac{h}{D_t})} = 1.658482734 - (1.658482734 - 0.001038592) \times e^{-0.3} = 0.430617914 \text{ m}$$

The velocity of the bubble rising in the column was then evaluated.

$$u_b = u_0 - u_{mf} + u_{br}$$

Where single bubble velocity is  $u_{br} = 0.71(gd_b)^{\frac{1}{2}}$

Equation 31: Bubble rise velocity

$$u_b = 0.065695938 - 0.013139188 + 0.71(9.81 \times 0.430617914)^{\frac{1}{2}} = 1.511837652 \text{ m/s}$$

The volume fraction of bubbles in the bed during normal operation could then be found.

$$\delta = \frac{u_0 - u_{mf}}{u_b - u_{mf}(1 + \alpha)}$$

Equation 32: Volume fraction of bubbles

Where the bubble wake parameter taken as  $\alpha = 0.4$ .

$$\frac{0.065695938 - 0.013139188}{1.511837652 - 0.013139188(1 + 0.4)} \delta = 0.035191673$$

The velocity of the solids was then evaluated.

$$u_s = \frac{\alpha \delta u_b}{1 - \delta - \alpha \delta}$$

Equation 33: Velocity of solids

$$u_s = 1 - \frac{0.4 \times 0.035191673 \times 1.511837652}{m} - 0.035191673 - 0.4 \times 0.035191673 = 0.022384485 \text{ m/s}$$

The velocity of the gas in the emulsion was also evaluated.

$$u_e = \frac{u_{mf}}{m_f} - u_s$$

Equation 34: Velocity of the emulsion phase

$$u_e = \frac{0.013139188}{0.500520555} - 0.022384485 = 0.00386656 \text{ m/s}$$

The rate constant was evaluated at operational temperature of 923.15K.

$$k = 2.03 \times 10^{21} \exp\left(-\frac{55300}{T}\right) \quad [15].$$

Equation 35: Rate constant for growth of polysilicon

$$k = 2.03 \times 10^{21} \exp\left(-\frac{55300}{923.15}\right) = 1.93851 \times 10^{-5} \text{ m/s}$$

Therefore, conversion could be found for the reactor by equation 22, and is tabulated below.

$$X = 1 - \exp\left(-\frac{hk}{u_o}\right)$$

Equation 36: Conversion in the fluidised bed reactor

$$X = 1 - \exp\left(-\frac{5 \times 1.93851 \times 10^{-5}}{0.065695938}\right) = 0.001474$$

Where conversion is defined as:

$$X = \frac{\text{moles of monosilane reacted}}{\text{moles of monosilane fed}}$$

And the molar ratio of monosilane to polysilicon is 1:1 given the stoichiometry of monosilane pyrolysis. Where moles of monosilane fed is taken from the mass balance specified for stream 94.

$$\begin{aligned} \text{moles of polysilicon deposited} &= (\text{moles of monosilane fed}) \times X = \left(\frac{1}{7} \times 0.05 \times \right. \\ &\left. \text{molar flow of monosilane} \right) \times \text{proportion of monosilane fed to reactor in sequence} \times \\ 0.001474 &= \frac{1}{7} \times \frac{u_o}{\sum_{\text{reactors}} u_o} \left( \times 0.05 \times 918.428738 \right) \times \quad \times 0.001474 \\ &= 0.073441 \text{ g/s} \\ \text{mass of polysilicon deposited} &= 0.002062223 \text{ g/s} \end{aligned}$$

Corresponding to a mass deposited across all 7 sets of 8 reactors as:

$$\text{mass of polysilicon deposited} = 0.4159867 \frac{\text{kg}}{\text{hr}}$$

Excel's Goal Seek function was then utilised to estimate the temperature at which the reactor must operate to deposit sufficient polysilicon and this reactor temperature was found to be 793.4 °C. This led to a corresponding conversion data shown below.

For the estimation regarding the column diameter, a sample number of columns were evaluated using a simplistic calculation based upon minimum fluidisation velocity to evaluate the dimensions of reactor and required quantities. Utilising the mass flow into the column in the vapour phase, the associated volumetric flowrate could be paired with required minimum fluidisation and corresponding operational fluidisation velocity for a given particle size to provide an estimate of the reactor diameter. The particle size was increased in stages from 100 microns to 1000 microns across a sequence of 8 reactors, with the maximum permissible reactor diameter of 5 m due to the consideration of a quartz lining to inhibit homogenous deposition [5]. The resulting number of reactors was found to be 56 operating across 7 sets of 8 sequential reactors, with diameter 5 m and an aspect ratio of 1.

Excel's solver feature was utilised to find minimum fluidisation velocity subject to Kunii & Levenspiel [11]. The minimum fluidisation velocity was found for the associated particle sizes, operational velocity taken as 5 times minimum fluidisation velocity and the fraction of flow through each reactor taken as a fraction of the total flow through all reactors. The surface area required for each set of fluidised bed reactors was found by volumetric flow across each set of reactors divided by the operational velocity of the reactors giving a corresponding cross sectional area, which could then be divided across a set number of reactors subject to the upper bound of individual reactor diameters of 5m. It was found that 7 sets of 8 reactors were sufficient.

Equation 37: Kunii and Levenspiel minimum fluidisation velocity equation utilised for solver calculations [11].

$$\frac{1.75}{\epsilon_{mf}^3 \phi_s} \left( \frac{d_p u_{mf} \rho_g}{\mu} \right)^2 + \frac{150(1 - \epsilon_{mf})}{\epsilon_{mf}^3 \phi_s^2} \left( \frac{d_p u_{mf} \rho_g}{\mu} \right) = \frac{d_p^3 \rho_g (\rho_s - \rho_g) g}{\mu^2} \quad (18)$$

Table 15: Shortcut design for diameter of reactor to achieve reactor diameters.

Inlet d <sub>p</sub>	outlet d <sub>p</sub>	Volume increase	Mass deposited	Fractional increase	u <sub>mf</sub>	u <sub>t</sub>	u <sub>o</sub>	u frac	Q Frac	Area of sum of FBR	diameter	Area per reactor	diameter
m	m	m <sup>3</sup>	kg		m/s	m/s	m/s			m <sup>2</sup>	m	m <sup>2</sup>	m
0.0001	0.000213	4.50E-12	1.05E-08	8.60E-03	0.042	5.56E-10	0.211	0.006	27.23	129.16	12.82	18.45	4.85
0.000213	0.000325	1.29E-11	3.02E-08	2.48E-02	0.186	2.51E-09	0.928	0.028	119.90	129.16	12.82	18.45	4.85
0.000325	0.000438	2.59E-11	6.03E-08	4.95E-02	0.410	5.87E-09	2.049	0.062	264.67	129.16	12.82	18.45	4.85
0.000438	0.00055	4.33E-11	1.01E-07	8.27E-02	0.677	1.06E-08	3.383	0.102	436.93	129.16	12.82	18.45	4.85
0.00055	0.000663	6.51E-11	1.52E-07	1.25E-01	0.951	1.68E-08	4.756	0.144	614.26	129.16	12.82	18.45	4.85
0.000663	0.000775	9.15E-11	2.13E-07	1.75E-01	1.214	2.44E-08	6.070	0.183	784.04	129.16	12.82	18.45	4.85
0.000775	0.000888	1.22E-10	2.85E-07	2.34E-01	1.458	3.34E-08	7.291	0.220	941.68	129.16	12.82	18.45	4.85
0.000888	0.001	1.58E-10	3.67E-07	3.01E-01	1.683	4.38E-08	8.413	0.254	1086.68	129.16	12.82	18.45	4.85



## Appendix B – Start-up, Shutdown and Normal Operation Sequences

Table 16: Start up process for the fluidised bed reactor

Unit	Stages
Milling	<ol style="list-style-type: none"> <li>1. Pre-start up checks e.g. check the equipment, valves etc.</li> <li>2. Start roller crusher and ball mill lubrication system and start to load MG-Si to the feed tank (10-TK-001).</li> <li>3. Open air valves to cyclones and cylinder operated valves, turn up the fan to introduce airflow to the dryer (10-H-001), start up the air recovery system.</li> <li>4. Open barren solution isolation valves to the feed pump box of cyclones and the barren solution shut off valves to ball mills. Open the gland water valve to let gland water flow to the cyclone feed pump.</li> <li>5. Switch density controller to MANUAL mode and set the desired output and setpoint. Then start the cyclone feed pump.</li> <li>6. Switch the flow controller to MANUAL mode and set a volumetric flow rate output (60% of controller output), then start the motors of the roller crusher and ball mills.</li> <li>7. Switch weight controller to MANUAL mode and set a lower output (20% of the controller output) at first, then gradually raise (2-3 min) the feed rate to a higher one (70% of the controller output). Then start the conveyor belt and start to feed MG-Si to the roller crusher (10-CR-001).</li> <li>8. When the desired output of the controllers has been achieved and other equipment is working smoothly, switch the weight controller to AUTO mode, then adjust the flow controller to fit the weight input when the weight controller is working stably, and switch the flow controller to AUTO mode.</li> </ol>
Turbomachinery	<ol style="list-style-type: none"> <li>1. The pre-commissioning and commissioning stages discussed earlier should ensure that all turbomachinery is ready for use.</li> <li>2. Pumps should be started by opening the inlet valve to allow fluid to flow in. The motor should then be started and the outlet valve gradually opened until the pump reaches its desired flowrate. [26]</li> <li>3. Once all pre-start-up checks have been completed, compressors should be turned on. Attention should be paid to both the suction and oil pressure to ensure the compressor is functioning correctly.</li> </ol>
Heat Exchangers	<ol style="list-style-type: none"> <li>1. Before adding process fluids, heat exchangers should be purged using an inert.</li> <li>2. The cooling fluid should be slowly added to the exchanger and the outlet stream opened once the shell/tubes are full.</li> <li>3. The hot stream should be added after the cold stream. An addition should be slow at first to allow the shell/tube to fill before opening the outlet.</li> </ol>
Fluidised Bed Reactor	<ol style="list-style-type: none"> <li>1. Purge reactor with nitrogen, preheated the heater to 250 °C, to remove all moisture from the inner lining of the reactor. Seed particles of silicon are heated in the furnace to an operational inlet temperature of 650°C, and the reactor jacket with heating fluid operated to maintain reactor temperature. Start feed of heated seed crystals of polysilicon into the reactor and</li> <li>2. increase the flow of preheated hydrogen gradually until the flow reaches operational velocity and thus the bed reaches a state of fluidisation. Once fluidisation is reached, the silane feed can be introduced to mix with the hydrogen in the mixing tank and the operation of the bed can function as required.</li> <li>3. Once mixed silane and hydrogen feed is introduced, the deposition will begin onto the seed crystals and continuous extraction of the product must begin once sufficient epitaxial growth has occurred.</li> </ol>



	<p>4. The cyclone must begin to separate any fines formed in the reactor but no mechanical duty is required for this to begin. Fines storage and collection must be constantly maintained to ensure no unattended build-ups of dust occur thus posing a safety risk.</p> <p>5. As extraction of the product from the reactor occurs, recovery of heat will begin from 50-E-003 when cooling polysilicon particles, and the recovery of smaller crystals will be made over separator 50-S-001.</p> <p>Additional Requirements: For the start-up of the silane fed FBR, there is a requirement of electronicgrade polysilicon to be utilised as seed particles.</p>
--	---

Plant Area	Unit	Comments	Estimated Time
------------	------	----------	----------------

Area 50	50-E-001/1/3/4/5	This is based on a literature reference [27]. The heat	30 minutes each
---------	------------------	--	-----------------

Table 17: Shutdown process for the fluidised bed reactor

Unit	Procedure
Milling	<ol style="list-style-type: none"> <li>1. Shut off the cyanide metering pump. Switch the weight controller to MANUAL mode and set the output to 0%, then run the roller crusher and ball mill for 30 minutes.</li> <li>2. Switch the density and flow controller to MANUAL mode and set the output to 0%.</li> <li>3. Turn off the lime timer of ball mills. Disengage the ball mill clutch, then the mill feed conveyer belts will stop automatically due to the interlocks. Turn off the convey belt and run the drier and air recovery system (including fans) for 30 minutes then turn them off.</li> <li>4. Shut down the motors of roller crusher and ball mills. Drain and flush the cyclone system, then shut off the cyclone feed pumps and close the gland seal water shut off valves to the cyclone feed pumps. Close the air block valves to the cyclones and the shut-off valves of all barren solution lines.</li> </ol>
Turbomachinery	<ol style="list-style-type: none"> <li>1. Pumps should be shut down by closing off the outlet and turning off the motor [13].</li> <li>2. Compressors are shut down by turning off their motors.</li> <li>3. The outlet streams from both pumps and compressors should be drained once shut down to prevent corrosion.</li> <li>4. Turbomachinery should be isolated once shut down to allow for maintenance.</li> </ol>
Heat Exchangers	<ol style="list-style-type: none"> <li>1. The flowrate of the hot stream should be reduced before that of the cold stream. This is done by gradually closing inlet valves.</li> <li>2. Once the inlet and outlet streams have been shut-off, the exchanger should be vented and purged.</li> </ol>
Fluidised Bed Reactor	<ol style="list-style-type: none"> <li>1. Reduce heating to seed/catalyst particles and reduce their flow into the reactor.</li> <li>2. Reduce the flowrate of feed gas by reduction of flow of monosilane.</li> <li>3. Reduce the flowrate of fluidisation gas.</li> <li>4. Once fluidisation of the bed has stopped, the solids are allowed to flow out of the bottom of the reactor, any particles large enough will be collected by the cyclone separator.</li> <li>5. Once all gas and particle streams have stopped, purge the system with heated inert in the same way as for start-up to ensure there is no remaining silane.</li> </ol>

Table 18: FBR plant time to steady state for main units

		exchanger is heated slowly of start-up to avoid thermal stresses.	
	50-R-001	56 reactors started in banks of 8 with each bank of reactors taking 42 minutes to reach steady state.	4.9 hours
	50-CR-001	The start-up operation of roller crusher and ball mill is assumed to be the same.	30 minutes each

	50-S-001/2	The gas flowrate is gradually increased until the required velocity is reached and the particles are suspended	15 minutes
--	------------	--	------------